SINGLE PARTICLE INCLUSIVE SPECTRA RESULTING FROM THE COLLISION OF RELATIVISTIC PROTONS, DEUTERONS AND ALPHA PARTICLES WITH NUCLEI[†]

J. Jaros, J. Papp, L. Schroeder, J. Staples,
H. Steiner, and A. Wagner*

Lawrence Berkeley Laboratory
University of California
Berkeley, California 94720

We have measured the yields of positive and negative particles resulting from the collision of 1.05 GeV/nucleon and 2.1 GeV/nucleon protons, deuterons and alpha particles with targets of Be, C, Cu, and Pb. Single particle inclusive spectra were obtained at 2.5° (lab) for $\pi^{\pm}$, K^{+}, p, d, ^{3}H, ^{3}He, and ^{4}He. In this paper we limit our discussion to those aspects of these spectra which are related to possible applications and tests of various high energy interaction models. In particular, we will indicate how our results bear on such concepts as limiting fragmentation, scaling, and the "parton" structure of the alpha particle and deuteron projectiles.

[†]Work done under the auspices of the United States Atomic Energy Commission.

*Permanent Address: Erstes Physikalisches Institut der Universität, Heidelberg, Germany.

We report here some preliminary results of an experiment to measure single particle inclusive spectra resulting from the collisions of 1.05-4.2 GeV (kinetic energy) protons, and 1.05 and 2.1 GeV/nucleon deuterons and alpha particles with targets of Be, C, Cu, and Pb. The yields of $\pi^{\pm}$, p, d, ^{3}H, ^{3}He, and ^{4}He were measured as a function of momentum at a fixed laboratory angle, $\theta = 2.5°$. The initial motivation for this experiment was to measure negative pion production from a variety of targets bombarded by relativistic deuterons and alpha particles to search for very energetic pions; pions with energies considerably larger than those which could be produced in a collision of a single nucleon with a nucleus. A second phase of the experiment consisted of reversing the polarity of our spectrometer and measuring positive particle yields. It was thought that the high energy fragmentation of deuterons and alpha particles might provide a heretofore unexploited means of studying particle momentum distributions and correlations inside these projectiles. It seemed quite possible that the fragmentation of these particles, even in the range of 1-2 GeV/nucleon, would already have reached some kind of limiting or asymptotic distribution, and that measurements of these fragmentation spectra might thus also afford rather interesting tests of such concepts as limiting fragmentation, scaling, and factorization. We were curious to see to what extent the various mechanisms proposed to describe very high energy elementary particle collisions could be applied to deuteron and alpha particle interactions at these energies. In this context, a series of questions present themselves:

(1) What is the role of diffractive dissociation, Regge or Pomeron exchange processes, multiperipheralism, fireballs, and other similar concepts in the collisions of high energy heavy ions with complex targets?

(2) Is there any relation between the characteristic energies of a system (e.g., the spacing of the energy levels) and the energy at which asymptotic considerations become valid?

(3) What can be learned about the "parton" structure of these particles in experiments of this type? After all we are dealing with systems whose nuclear structure is thought to be reasonably well understood, and so we should be able to test some of these ideas in a more familiar context, namely, the decomposition of a nuclear particle into its constituents.

Although we cannot answer all of these questions completely with the data presented here, we would like to indicate how our measurements bear on some of these concepts.

The experiment was performed in the external beam of the Bevatron. Fluxes of particles ranged from 10^9-10^{10} per pulse for alphas, and 10^{10}-10^{11} per pulse for deuterons. A double focusing spectrometer was used to momentum analyze the secondary particles and to transmit them to our detecting system. The detection system was extremely simple, consisting of two scintillation counters to measure the time-of-flight of the secondaries over a 15 meter flight path, and a pair of scintillation counters to record their pulse heights and in this way to distinguish between singly and doubly charged particles. The time-of-flight spectra were stored in a 400 channel

analyzer and then read onto magnetic tape. Data were typically taken at momentum/charge intervals of 0.25 GeV/c over the range, $0.5 \leq k \leq 5.0$ GeV/c. No attempts were made to make measurements below 0.5 GeV/c because in the case of pions the lepton contamination and the decay corrections became too large to be easily manageable. For protons and heavier fragments the multiple scattering and energy loss considerations made it impracticable to go to lower momenta. The upper limit of 5 GeV/c was set by limitations on the current in the magnets of the beam transport system. A monitor telescope (three scintillation counters in coincidence) was placed about 3 meters from the production targets at about 90° to the incident beam. The monitor counts, which were proportional to the amount of beam striking a given target, were used during the experiment as a relative normalization for our yields. To obtain an absolute normalization the monitor counts for each target were periodically calibrated against the beam intensity as measured with both an ionization chamber and a secondary emission monitor which were located in the primary beam just upstream of the production targets. Some unresolved questions still exist about these calibrations, and also about the effective solid angle acceptance of our spectrometer, so that the absolute normalization of our particle yields are not final. The momentum dependence of these yields for each target is not affected by these uncertainties. During the course of running, a scintillation screen viewed by a TV camera was moved into the beam to check the spot size of the beam at our production target and to see that the beam had not wandered off the target.

We turn first to the results on negative pion production. In Fig. 1 we show the single particle inclusive π^- spectra at 2.5° (Lab) resulting from the collision of 1.05, 1.73, 2.10, 2.60, 3.50, and 4.20 GeV protons

with a 0.64 cm long Be target. Similar spectra, not shown here, were obtained with C, Cu, and Pb targets. In these spectra as well as in all of the other pion yields to be reported here the results were corrected for lepton contamination in the beam (as measured with a gas-filled Cherenkov counter), decay in flight, and effects due to the finite lengths of the targets used. Except for the points at the very tails of these distributions the statistical errors are very small, and do not constitute the major uncertainty in our results. Systematic effects due to focusing and steering the primary beams onto our targets constituted the main source of error outside of the aforementioned monitor calibration problems. When these results are replotted in terms of the Lorentz Invariant cross se tion $\frac{E}{k^2}\frac{d^2\sigma}{d\Omega dk}$ versus the scaling variable $x' = \frac{k_{\parallel}^*}{(k_{\parallel}^*)_{max}}$ (where $k_{\parallel}^*$ is the longitudinal momentum of the outgoing pion as measured in the overall center-of-mass system) a rather remarkable result appears (Fig. 2). All of the spectra tend to fall on top of each other. This scaling property, where the pion yield becomes a function only of the single scaling variable x', usually at a fixed $k_\perp$ and independent of the total energy, is familiar at higher energies, but here we see that even at 1 GeV the scaling behavior is quite well satisfied. It should be kept in mind that because the experiment was done at a fixed angle in the laboratory system ($\theta_L = 2.5°$) the transverse momentum, $k_\perp$, is not strictly constant ($22 \leq k_\perp \leq 220$ MeV/c). However, especially at the lower momenta $k_\perp$ stays small and does not vary much in an absolute sense. At the higher momenta (e.g. 3-4 GeV/c) this variation of $k_\perp$ may well be responsible for the observed differences in the various spectra.

The laboratory cross section, $\frac{d^2\sigma}{d\Omega dk}$, as a function of pion momentum,

k, for pion production by 1.05 GeV/nucleon and 2.10 GeV/nucleon protons, deuterons, and alpha particles on Be is shown in Figs. 3 and 4. Two features stand out:

1) Pions are produced more copiously by deuterons and alphas than by protons, and
2) The pion spectra induced by deuterons and alphas extend to higher momenta than those induced by protons.

Preliminary attempts to fit the observed deuteron and alpha induced pion production spectra with a model in which the nucleons moving inside the projectile collide individually and independently with the target nucleus seem to reproduce the qualitative features of the spectra.

The Lorentz Invariant cross sections $\frac{E}{k^2}\frac{d^2\sigma}{d\Omega dk}$ vs x' for pion production by deuterons and alpha particles is shown in Figs. 5 and 6. Again the scaling property of these distributions seems to be satisfied. It is also interesting to note that these distributions fall much more steeply with x' as the mass of the projectile is increased. This feature is not unexpected since a complicated loosely-bound object like an alpha particle probably has a much harder time transferring a large fraction of its energy to a single pion than does a proton.

In Fig. 7 we show the pion yield as a function of laboratory momentum for 2.1 GeV/nucleon alpha particles on various targets. It is seen that the shape of these spectra is almost independent of target material. This feature is true of all the pion spectra measured in this experiment, except at the very lowest mementa where a slight target dependence becomes noticeable. As shown in Fig. 8 the pion production

cross sections for 2.1 GeV/nucleon alpha particles (as well as those for other projectiles and energies) are proportional to $A^{1/3}$ when $k \gtrsim 1$ GeV/c.

Next we turn to our results on the fragmentation of protons, deuterons, and alpha particles into positively charged particles. A large amount of data was amassed (incident energies: 1.05 and 2.10 GeV/nucleon; incident particles: protons, deuterons and alpha particles; targets: Be, C, CH_2, Cu, Pb, fragments: π^+, p, d, ^{3}H, ^{3}He, ^{4}He.) As an example in Fig. 9 is shown the fragmentation of 1.05 GeV/nucleon alpha particles by a Be target. The "parton" structure of the alpha particle is clearly displayed. Not only does ^{4}He consist of proton and neutron constituents, but also deuterons, ^{3}H, and ^{3}He. We thus expect that high energy diffractive dissociation of alpha particles in reactions of this type should provide us with a reasonable clean "snapshot" of nucleon correlations and momentum distributions without having the interaction itself seriuosly disturb the pre-existing conditions in the projectile. Care should be exercised in interpreting the magnitudes of the various peaks, because as has been pointed out previously the data were taken at fixed $\theta_{lab} = 2.5°$, and consequently different transverse momenta are involved in these distributions. These effects can be significant since typical Fermi momenta are 100 to 200 MeV/c and at $\theta_{lab} = 2.5°$ a k = 2 GeV/c particle has a transverse momentum of ~100 MeV/c. In any case, it is evident that the fragmentation of ^{4}He into deuterons has a cross section comparable to that for fragmentation into protons. It should also be noted that the position of the proton, deuteron, and ^{3}H, ^{3}He peaks occur as expected at one-fourth, one-half,

and three-fourths of the momentum of the incident alpha particle. These facts are neatly summarized in a plot of the Lorentz Invariant cross section $\frac{E}{k^2}\frac{d^2\sigma}{d\Omega dk}$ versus y_c, the rapidity of the outgoing fragment. Such a plot is shown in Fig. 10. Several features stand out:

1) The peaks of the rapidity distributions all coincide with the rapidity of the incident alpha particle projectile.
2) The heavier the fragment the more sharply peaked (i.e., the narrower) the distribution.
3) The diffractive dissociation peak is cleanly separated from other identifiable regions of the rapidity distribution, i.e., it is well separated from the rapidity of the target, and stands out clearly from the central ("pionization") region. Again, this feature is not unexpected. On the contrary it would be surprising to find large numbers of these fragments in the central region, and the bulk of the particles resulting from target fragmentation are too low in momentum to be detected by our detecting system.
4) Because of the 0.5 GeV/c lower limit on the momentum of particles detected in this experiment the rapidity distribution of the pions (because of their small mass) extends to much higher values of rapidity than do the distributions of the heavy fragments.

In Figs. 11 and 12 are shown the laboratory cross sections and the Lorentz Invariant rapidity distributions resulting from the fragmentation of 1.05 GeV/nucleon deuterons on Be. The momentum distribution of the protons is again centered at the same point as in the case of the alpha particle, but here the distribution is significantly narrower. This is not unreasonable since the deuteron is a much more loosely bound system

than ^{4}He. This can also be seen by comparing the rapidity distributions. The shape of the deuteron spectrum is reminiscent of other inelastic scattering processes, and it may well be that rather similar theoretical considerations apply to all of these processes.

Finally, in Figs. 13 and 14 are presented the laboratory cross sections and the Lorentz Invariant rapidity distributions of protons resulting from the fragmentation of 2.1 GeV/nucleon deuterons and alpha particles by Be. Again the protons from the alpha fragmentation have a broader momentum (and rapidity) distribution than do the protons from deuteron disintegration. At first sight a comparison of Figs. 10, 12, and 14 would seem to indicate that these proton distributions have not yet attained any kind of limiting characteristic, but here again the pitfall of measurements at a fixed laboratory angle must be taken into account. Although a definitive statement about limiting distributions in this case must await further experimental investigation, it seems likely that the observed distributions are indeed at some kind of asymptotic limit.

Lack of space and time prevents us from showing the detailed behavior of these distributions for different targets. In practically all cases, however, the shapes of the distributions shown above for the case of Be are almost identical to those of the other targets. Only in the case of very low momentum heavy fragments do target dependent effects manifest themselves.

In this paper we have tried to show that single particle inclusive spectra resulting from the interactions of relatively modest-energy protons, deuterons, and alpha particles with nuclear targets show many of the features

such as scaling and limiting fragmentation that are characteristic of very high energy elementary particle interactions, and that experiments of the type discussed here may shed additional light not only on the nuclear physics aspects of these reactions but also on possible high energy interaction mechanisms.

We thank Dr. Hermann Grunder and the Bevatron Staff for their important contributions to this experiment. We also thank J. Wiss for help with the data analysis.

FIGURE CAPTIONS

Figure 1. $\left(\frac{d^2\sigma}{d\Omega dk}\right)_{lab}$ for π^- production by protons on Be as a function of pion momentum. θ = 2.5° (lab). The different points correspond to different proton energies. The curves have no theoretical significance and were drawn only to aid the eye in connecting the points at each energy.

Figure 2. π^- production by protons on Be. θ = 2.5° (lab). The data of Fig. 1 plotted in terms of the Lorentz Invariant cross section $\frac{E}{k^2}\frac{d^2\sigma}{d\Omega dk}$ vs the scaling variable $x' = \frac{k_{\parallel}^*}{(k_{\parallel}^*)_{max}}$.

Figure 3. $\left(\frac{d^2\sigma}{d\Omega dk}\right)_{lab}$ for π^- production by 1.05 GeV/nucleon protons, deuterons, and alphas on Be. θ = 2.5° (lab).

Figure 4. $\left(\frac{d^2\sigma}{d\Omega dk}\right)_{lab}$ for π^- production by 2.10 GeV/nucleon protons, deuterons, and alphas on Be. θ = 2.5° (lab)

Figure 5. The Lorentz Invariant cross section $\frac{E}{k^2}\frac{d^2\sigma}{d\Omega dk}$ vs the scaling variable $x' = \frac{k_{\parallel}^*}{(k_{\parallel}^*)_{max}}$ for pion production by 1.05 GeV/nucleon and 2.1 GeV/nucleon deuterons. θ = 2.5° (lab).

Figure 6. The Lorentz Invariant cross section $\frac{E}{k^2}\frac{d^2\sigma}{d\Omega dk}$ vs the scaling variable $x' = \frac{k_{\parallel}^*}{(k_{\parallel}^*)_{max}}$ for pion production by 1.05 GeV/nucleon and 2.1 GeV/nucleon alphas. θ = 2.5° (lab).

Figure 7. $\left(\frac{d^2\sigma}{d\Omega dk}\right)_{lab}$ vs pion momentum k for π^- production by 2.1 GeV/nucleon alpha particles for three different targets: Be, C, and Pb. θ = 2.5° (lab)

Figure 8. $\left(\frac{d^2\sigma}{d\Omega dk}\right)_{lab}$ vs A_{Target} for π^- production by 2.10 GeV/nucleon alpha particles for different pion momenta. $\theta = 2.5°$ (lab).

Figure 9. Fragmentation cross sections, $\left(\frac{d^2\sigma}{d\Omega dk}\right)_{lab}$, vs fragment momentum for dissociation of 1.05 GeV/nucleon alpha particles into protons, deuterons, ^3H, ^3He, and ^4He. $\theta = 2.5°$ (lab). Be target.

Figure 10. The data of Fig. 9 plotted in terms of the Lorentz Invariant cross section $\frac{E}{k^2}\frac{d^2\sigma}{d\Omega dk}$ vs the rapidity variable y_c. Arrows indicate the rapidity of the target and the incident alpha particle projectile. $\theta = 2.5°$ (lab).

Figure 11. Proton and deuteron production cross sections $\left(\frac{d^2\sigma}{d\Omega dk}\right)_{lab}$ vs fragment momentum resulting from the interaction of 1.05 GeV/nucleon deuterons in Be. $\theta = 2.5°$ (lab).

Figure 12. The data of Fig. 11 replotted in terms of the Lorentz Invariant cross section $\frac{E}{k^2}\frac{d^2\sigma}{d\Omega dk}$ vs the rapidity variable y_c.

Figure 13. Fragmentation cross sections $\left(\frac{d^2\sigma}{d\Omega dk}\right)_{lab}$ vs momentum for protons resulting from 2.10 GeV/nucleon deuteron and alpha particle interactions in Be. $\theta = 2.5°$ (lab).

Figure 14. The data of Fig. 13 replotted in terms of the Lorentz Invariant cross section $\frac{E}{k^2}\frac{d^2\sigma}{d\Omega dk}$ vs the rapidity variable y_c.

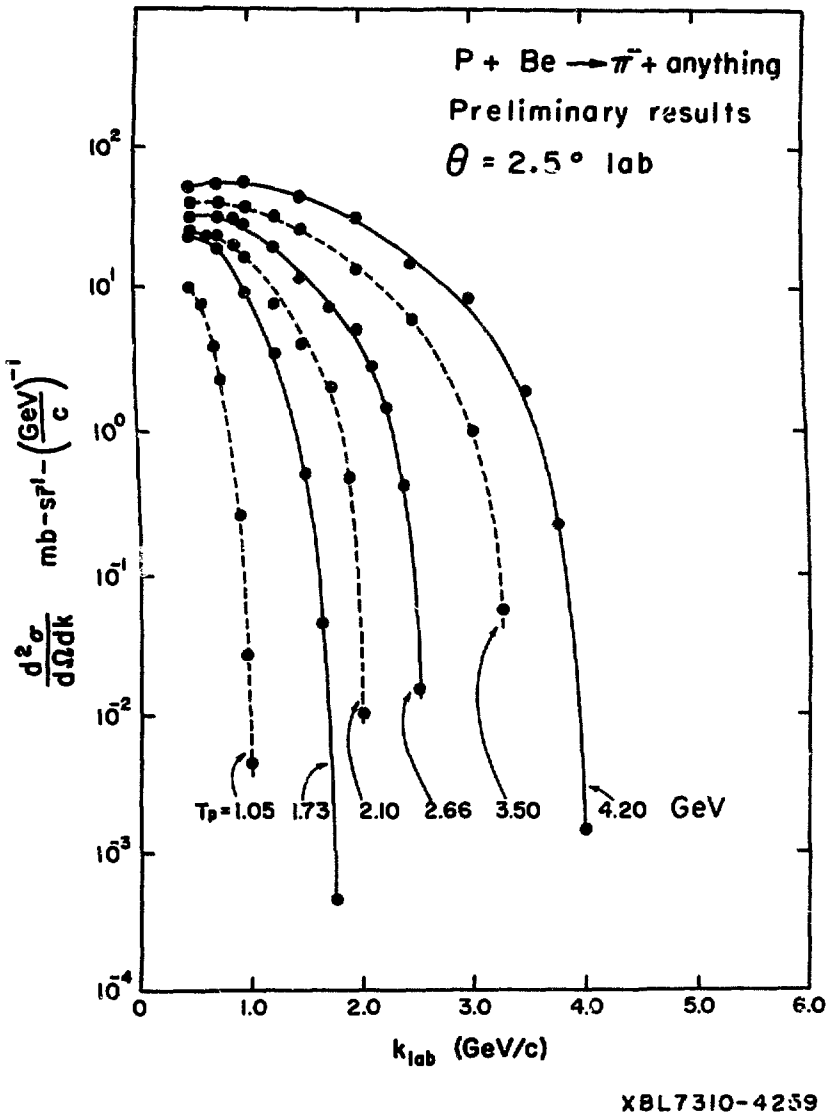
P + Be → π⁻ + anything
Preliminary results
θ = 2.5° lab
$\frac{d^2\sigma}{d\Omega dk}$ mb-sr^{-1}-$\left(\frac{GeV}{c}\right)^{-1}$
10^2
10^1
10^0
10^{-1}
10^{-2}
10^{-3}
10^{-4}
T_p=1.05 1.73 2.10 2.66 3.50 4.20 GeV
0 1.0 2.0 3.0 4.0 5.0 6.0
k_{lab} (GeV/c)
XBL7310-4259

Fig. 1.

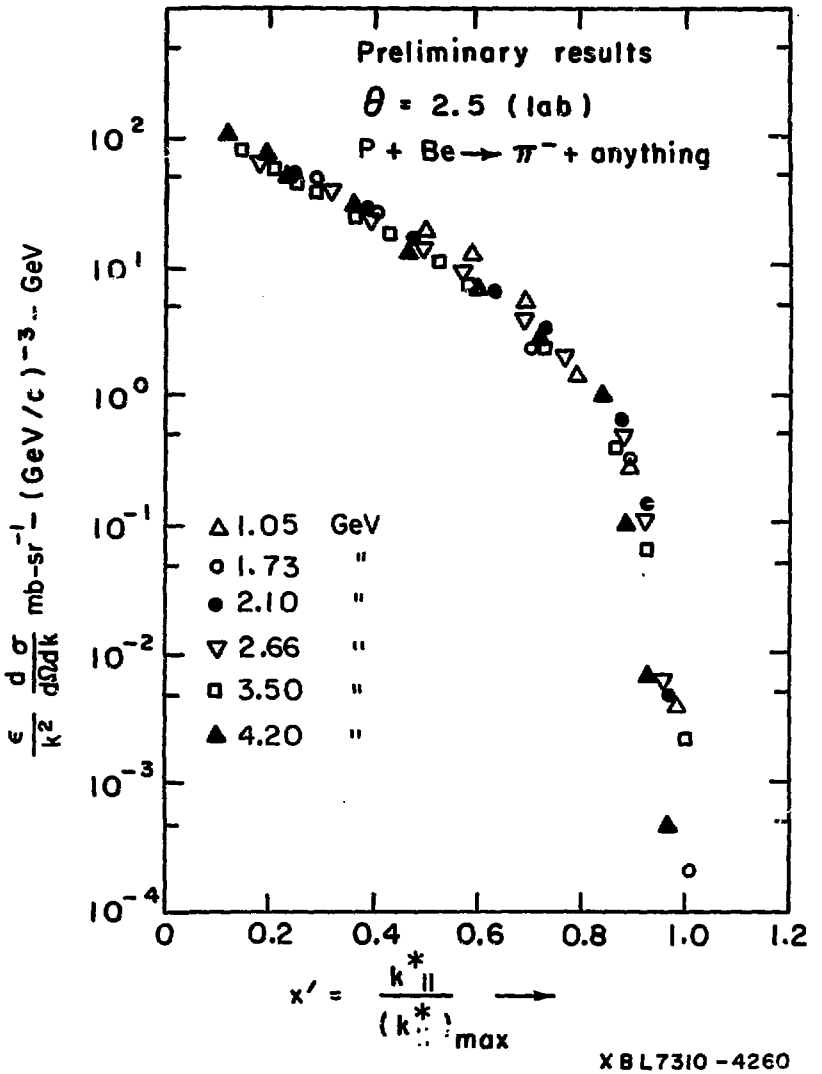
Preliminary results
θ = 2.5 (lab)
P + Be → π⁻ + anything
△ 1.05 GeV
○ 1.73 "
● 2.10 "
▽ 2.66 "
□ 3.50 "
▲ 4.20 "
$\frac{\epsilon}{k^2}\frac{d\sigma}{d\Omega dk}$ mb-sr^{-1}-(GeV/c)$^{-3}$-- GeV
$x' = \frac{k^*_{\parallel}}{(k^*_{\parallel})_{max}}$
XBL7310-4260

Fig. 2.

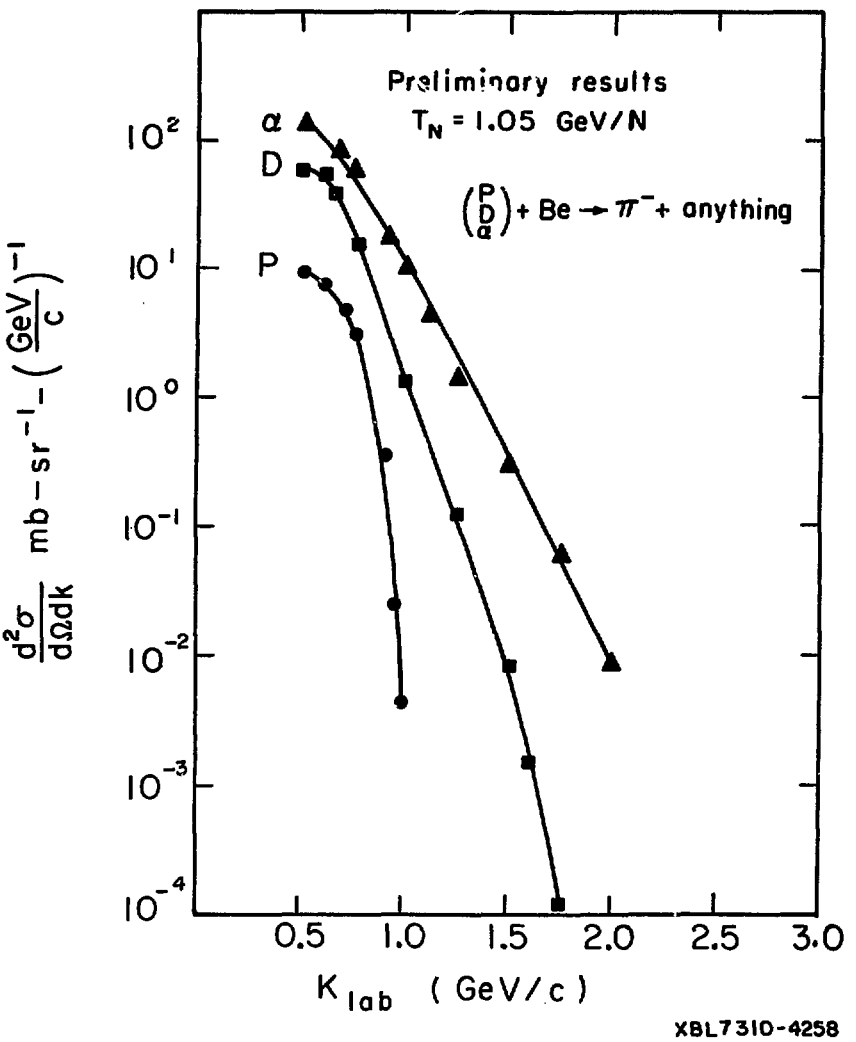
Preliminary results
T_N = 1.05 GeV/N
$\begin{pmatrix} p \\ D \\ \alpha \end{pmatrix}$ + Be → π^- + anything
α
D
P
10^2
10^1
10^0
10^{-1}
10^{-2}
10^{-3}
10^{-4}
$\frac{d^2\sigma}{d\Omega dk}$ mb − sr^{-1} − $\left(\frac{GeV}{c}\right)^{-1}$
0.5
1.0
1.5
2.0
2.5
3.0
K_{lab} (GeV/c)
XBL7310-4258

Fig. 3.

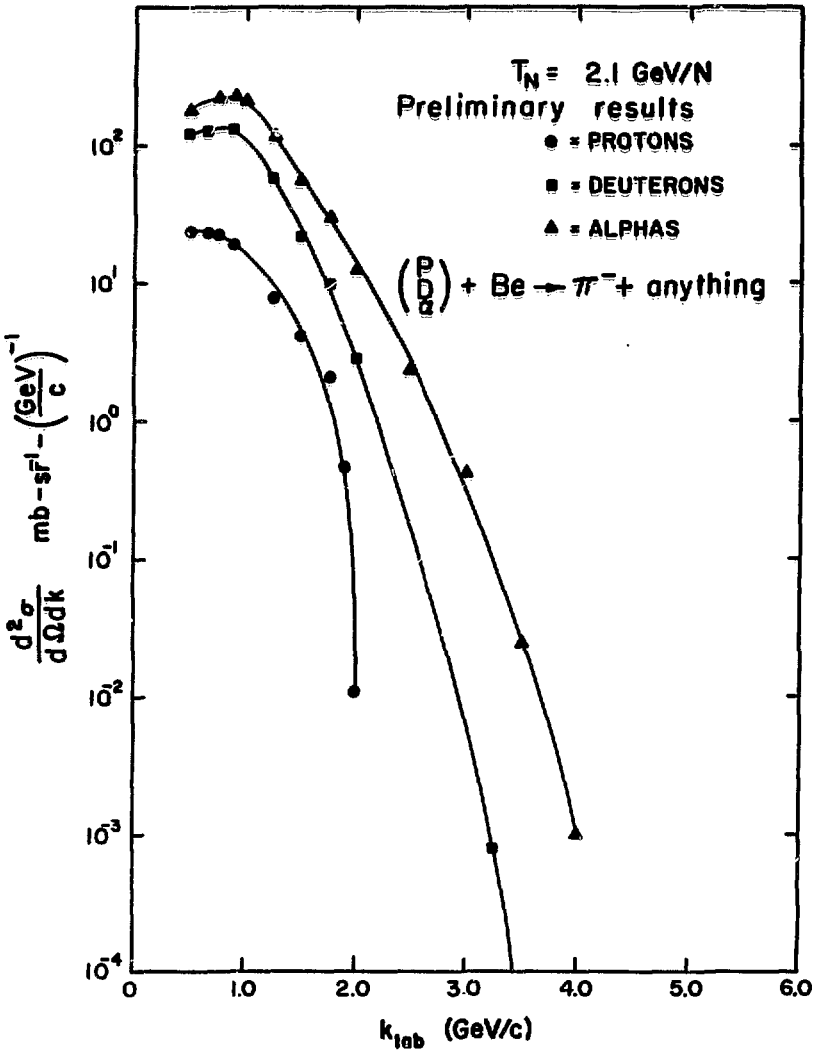
T_N = 2.1 GeV/N
Preliminary results
● = PROTONS
■ = DEUTERONS
▲ = ALPHAS
$\left(\frac{P}{D}_{\alpha}\right)$ + Be → π^- + anything
$\frac{d^2\sigma}{d\Omega dk}$ mb-sr^{-1}-$\left(\frac{GeV}{c}\right)^{-1}$
10^2
10^1
10^0
10^{-1}
10^{-2}
10^{-3}
10^{-4}
0
1.0
2.0
3.0
4.0
5.0
6.0
k_{lab} (GeV/c)
XBL7310-4261

Fig. 4.

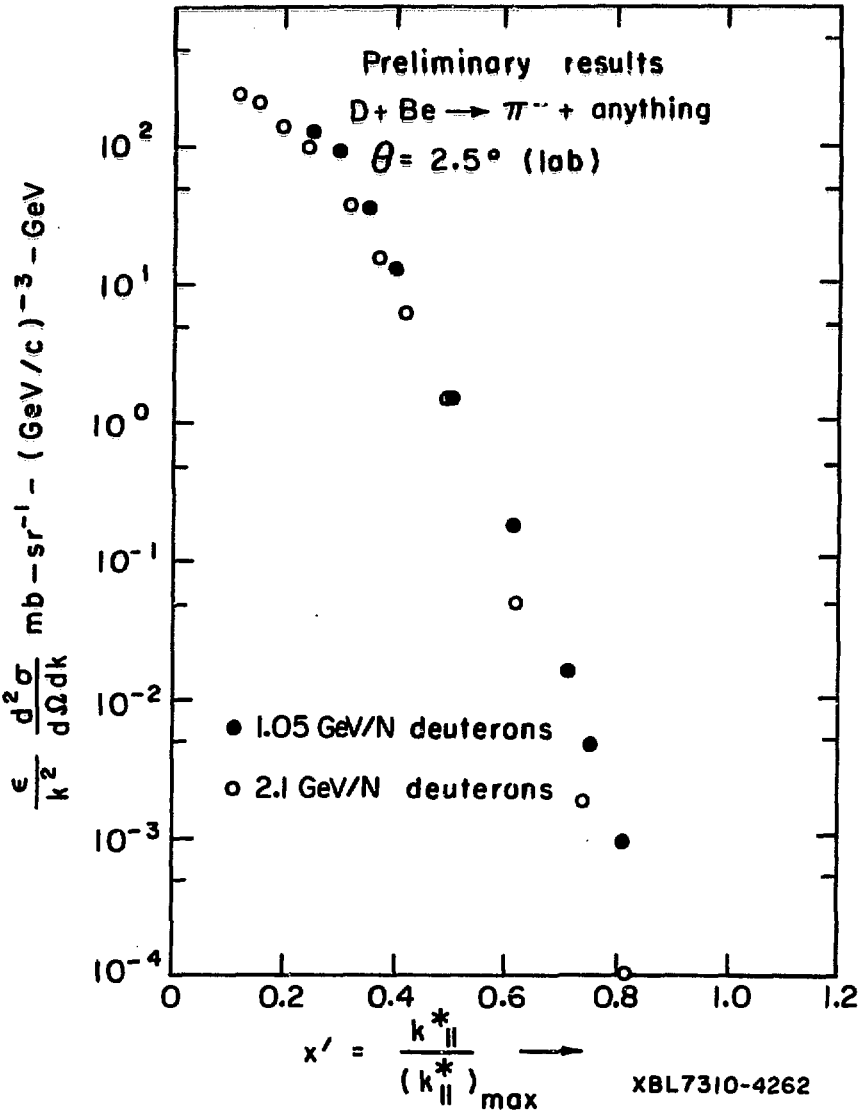
Preliminary results
D+ Be → π⁻ + anything
θ = 2.5° (lab)
● 1.05 GeV/N deuterons
○ 2.1 GeV/N deuterons
$\frac{\epsilon}{k^2}\frac{d^2\sigma}{d\Omega dk}$ mb−sr⁻¹ − (GeV/c)⁻³ − GeV
10^2
10^1
10^0
10^{-1}
10^{-2}
10^{-3}
10^{-4}
0
0.2
0.4
0.6
0.8
1.0
1.2
$x' = \frac{k^*_{\parallel}}{(k^*_{\parallel})_{max}}$ →
XBL7310-4262

Fig. 5.

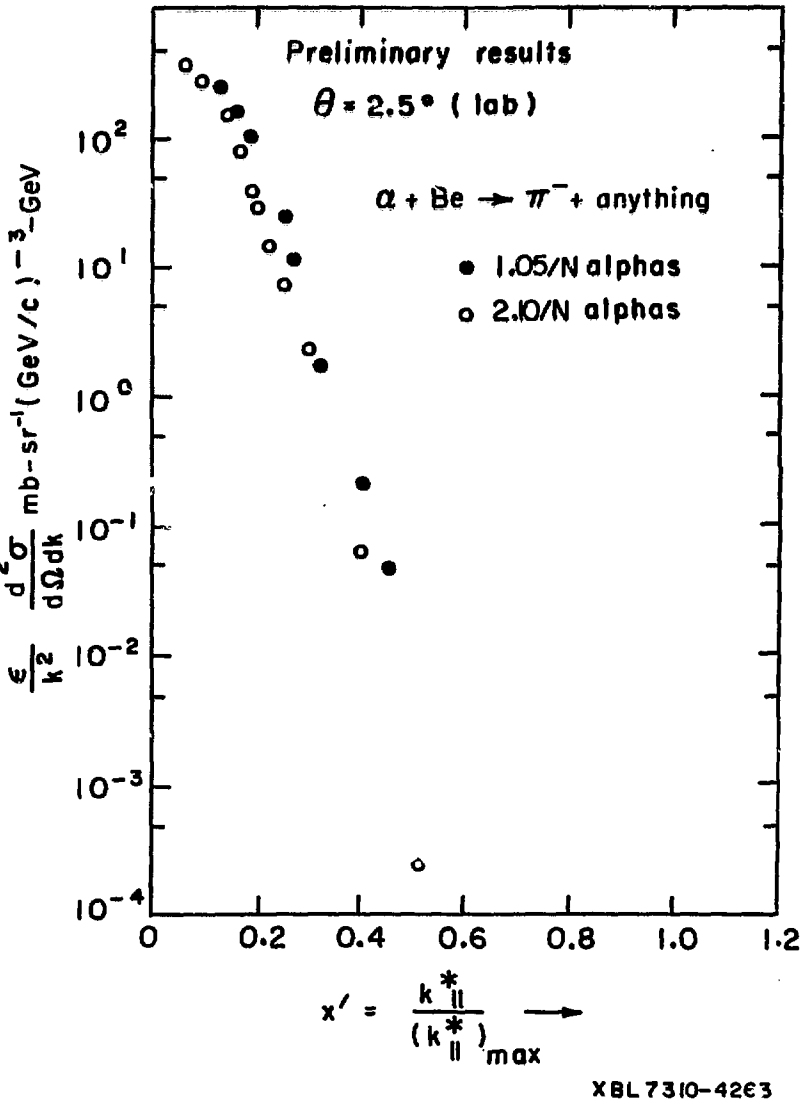
Preliminary results
θ = 2.5° (lab)
α + Be → π⁻ + anything
● 1.05/N alphas
○ 2.10/N alphas
$\frac{\epsilon}{k^2}\frac{d^2\sigma}{d\Omega dk}$ mb-sr⁻¹(GeV/c)⁻³-GeV
10²
10¹
10⁰
10⁻¹
10⁻²
10⁻³
10⁻⁴
0
0.2
0.4
0.6
0.8
1.0
1.2
$x' = \frac{k^*_{\parallel}}{(k^*_{\parallel})_{max}}$
XBL 7310-4263

Fig. 6.

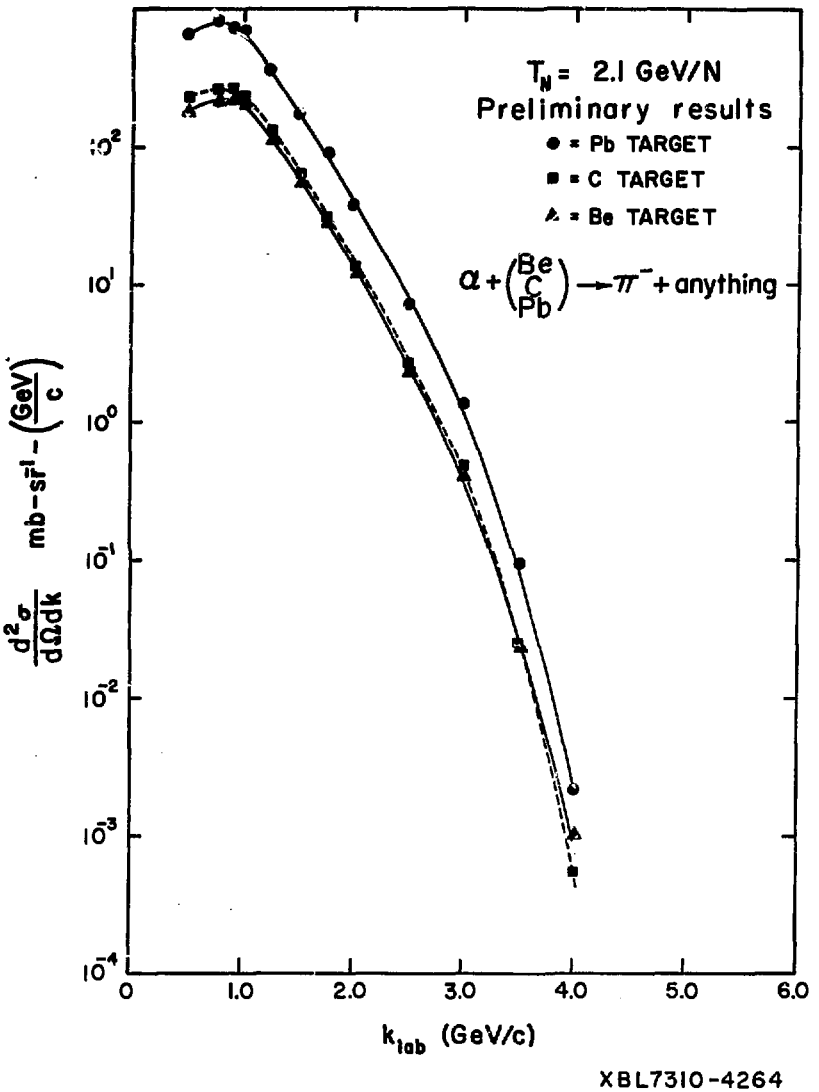
T_N = 2.1 GeV/N
Preliminary results
● = Pb TARGET
■ = C TARGET
▲ = Be TARGET
$\alpha + \begin{pmatrix} Be \\ C \\ Pb \end{pmatrix} \rightarrow \pi^- +$ anything
$\frac{d^2\sigma}{d\Omega dk}$ mb-sr^{-1}-$\left(\frac{GeV}{c}\right)^{-1}$
10^2
10^1
10^0
10^{-1}
10^{-2}
10^{-3}
10^{-4}
0
1.0
2.0
3.0
4.0
5.0
6.0
k_{lab} (GeV/c)
XBL7310-4264

Fig. 7.

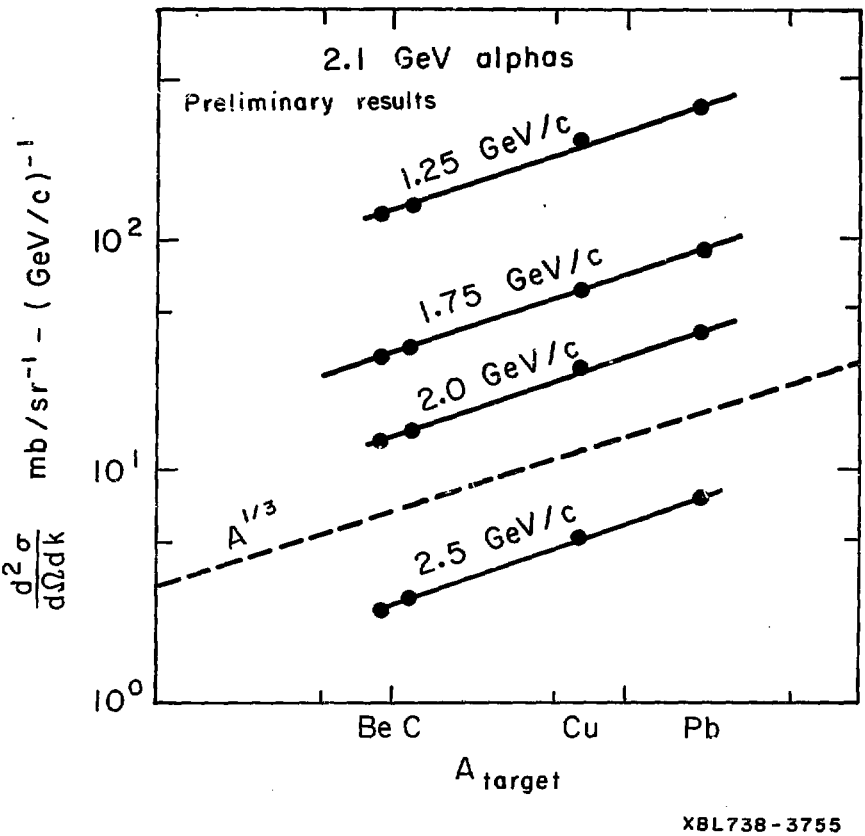
2.1 GeV alphas
Preliminary results
1.25 GeV/c
1.75 GeV/c
2.0 GeV/c
2.5 GeV/c
A^1/3
10^2
10^1
10^0
d²σ/dΩdk mb/sr⁻¹ - (GeV/c)⁻¹
Be C
Cu
Pb
A target
XBL738-3755

Fig. 8.

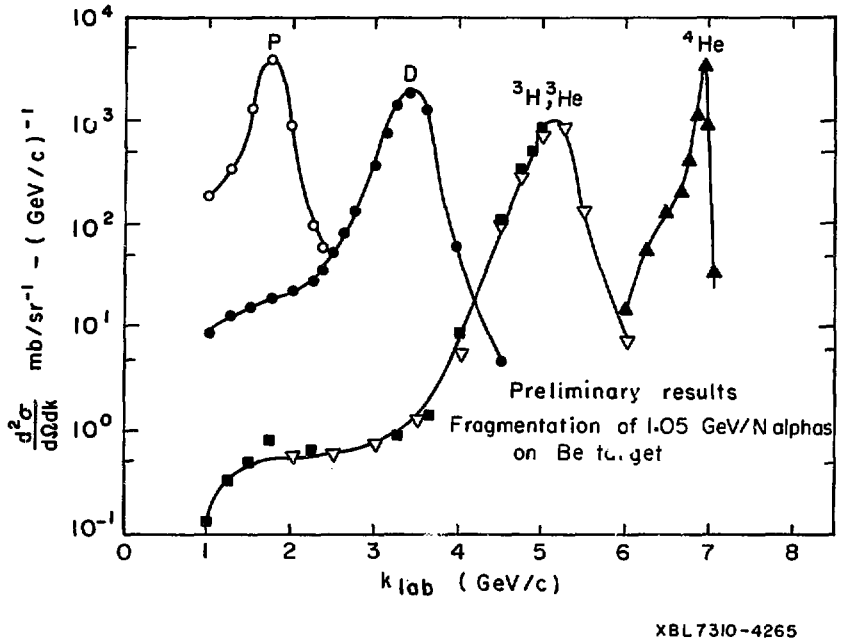
P
D
^{3}H;^{3}He
^{4}He
Preliminary results
Fragmentation of 1.05 GeV/N alphas
on Be target
$\frac{d^2\sigma}{d\Omega dk}$ mb/sr^{-1} - (GeV/c)$^{-1}$
k_{lab} (GeV/c)
XBL7310-4265

Fig. 9.

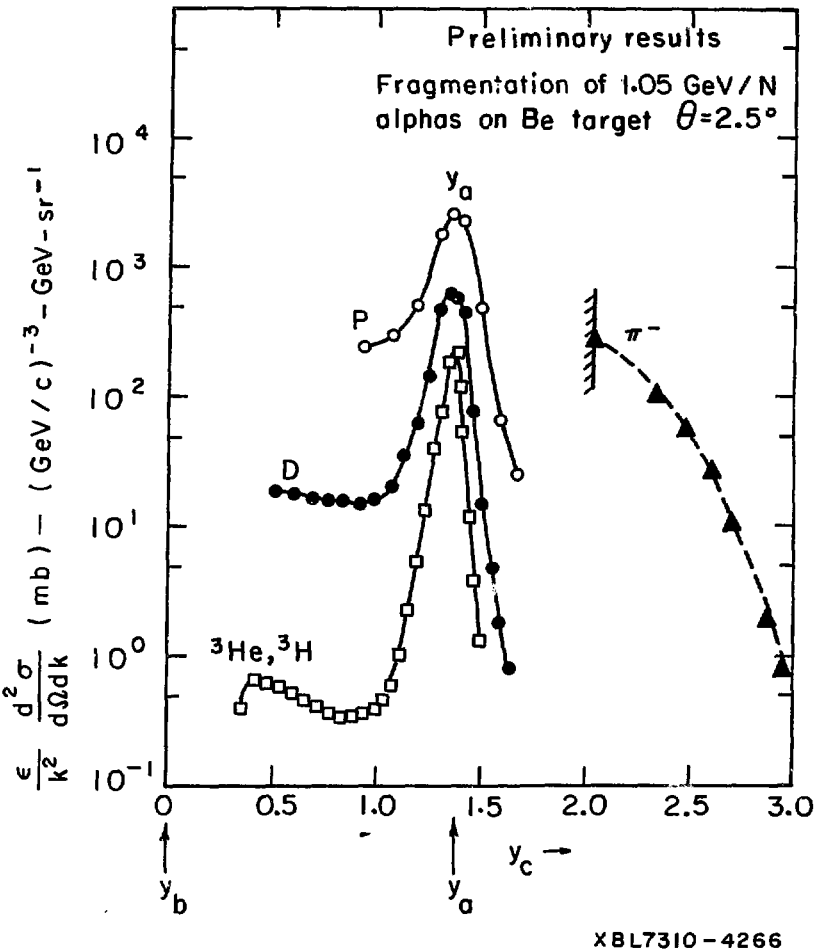
Preliminary results
Fragmentation of 1.05 GeV/N
alphas on Be target θ=2.5°
$\frac{\epsilon}{k^2}\frac{d^2\sigma}{d\Omega dk}$ (mb) — (GeV/c)$^{-3}$-GeV-sr^{-1}
10^4
10^3
10^2
10^1
10^0
10^{-1}
y_a
P
D
^{3}He,^{3}H
π^-
0
0.5
1.0
1.5
2.0
2.5
3.0
y_c →
y_b
y_a
XBL7310-4266

Fig. 10.

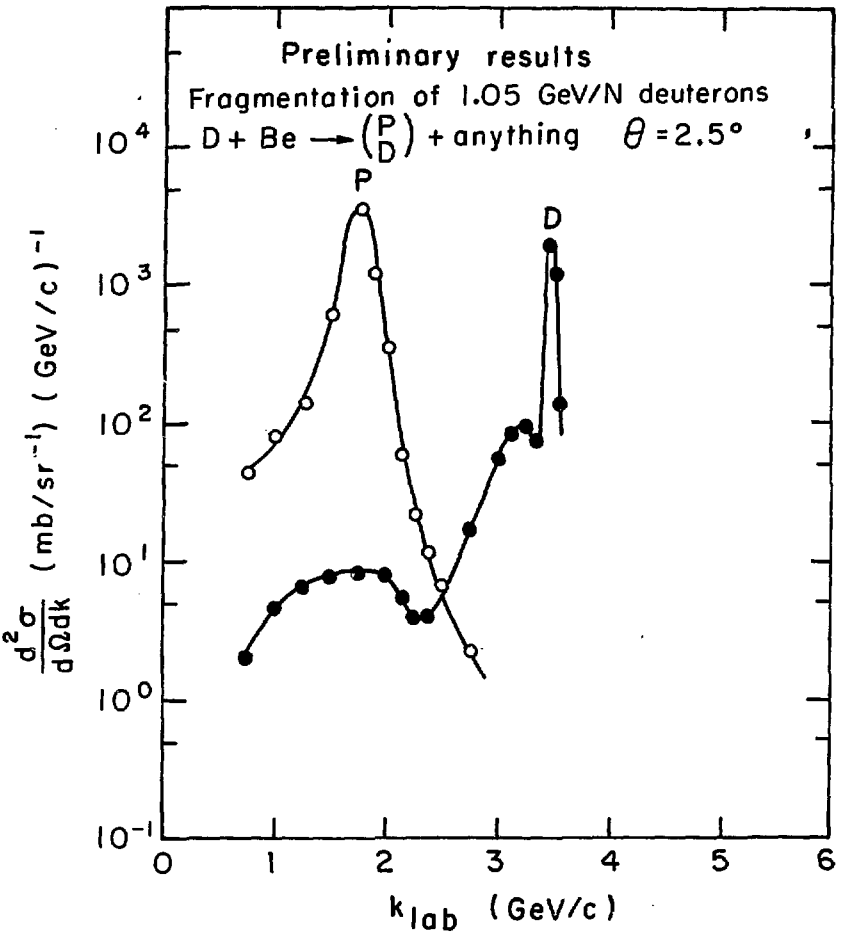
Preliminary results
Fragmentation of 1.05 GeV/N deuterons
D + Be → (P, D) + anything θ = 2.5°
P
D
$\frac{d^2\sigma}{d\Omega dk}$ (mb/sr^{-1}) (GeV/c)$^{-1}$
10^4
10^3
10^2
10^1
10^0
10^{-1}
0
1
2
3
4
5
6
k_{lab} (GeV/c)
XBL 7310-4267

Fig. 11.

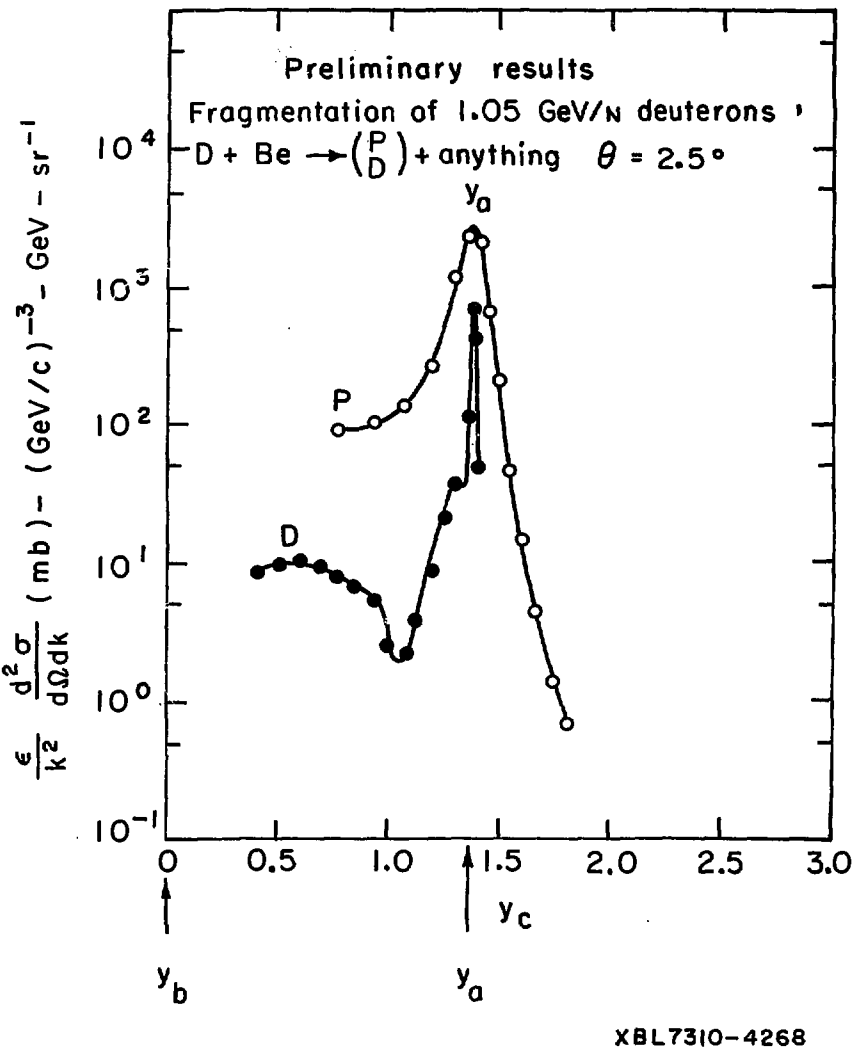
Preliminary results
Fragmentation of 1.05 GeV/N deuterons
D + Be → (P/D) + anything θ = 2.5°
$\frac{\epsilon}{k^2}\frac{d^2\sigma}{d\Omega dk}$ (mb) - (GeV/c)$^{-3}$ - GeV - sr^{-1}
10^4
10^3
10^2
10^1
10^0
10^{-1}
P
D
y_a
0
0.5
1.0
1.5
2.0
2.5
3.0
y_b
y_c
y_a
XBL7310-4268

Fig. 12.

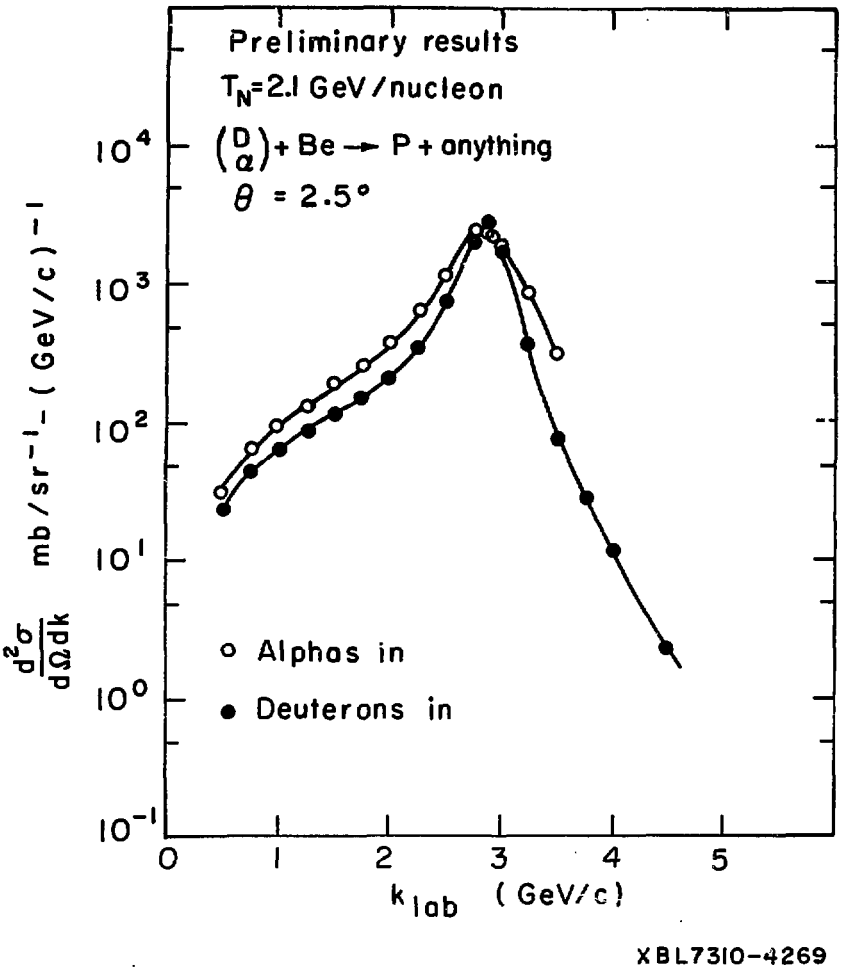
Preliminary results
T_N=2.1 GeV/nucleon
$\left(\frac{D}{\alpha}\right)$ + Be → P + anything
θ = 2.5°
$\frac{d^2\sigma}{d\Omega dk}$ mb/sr^{-1} (GeV/c)$^{-1}$
10^4
10^3
10^2
10^1
10^0
10^{-1}
o Alphas in
• Deuterons in
0
1
2
3
4
5
k_{lab} (GeV/c)
XBL7310-4269

Fig. 13.

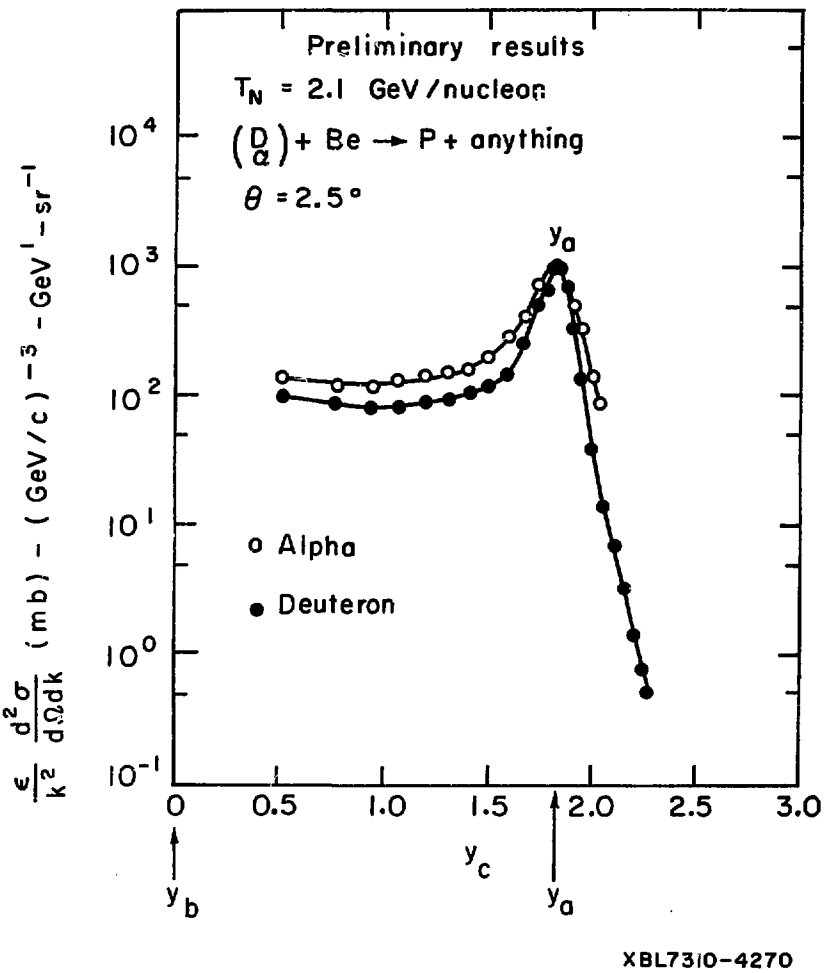
Preliminary results
T_N = 2.1 GeV/nucleon
$\left(\frac{D}{\alpha}\right)$ + Be → P + anything
θ = 2.5°
y_a
o Alpha
● Deuteron
$\frac{\epsilon}{k^2}\frac{d^2\sigma}{d\Omega dk}$ (mb) - (GeV/c)$^{-3}$ - GeV^{-1} - sr^{-1}
10^4
10^3
10^2
10^1
10^0
10^{-1}
0
0.5
1.0
1.5
2.0
2.5
3.0
y_b
y_c
y_a
XBL7310-4270

Fig. 14.